

**Synaptogyrin-dependent modulation of synaptic neurotransmission in
*Caenorhabditis elegans***

Abbreviated title: Synaptogyrin-dependent neurotransmission

Christian Abraham*, Lin Bai*, and Rudolf E. Leube*¹

*Institute of Molecular and Cellular Anatomy
RWTH Aachen University
Wendlingweg 2
52074 Aachen, Germany

¹Corresponding author:

Tel: ++49 241 8089107

Fax: ++49 241 8082508

Email: rleube@ukaachen.de

Number of figures and tables: 8 figures; 2 tables

Number of pages: 21

Number of words:

- Abstract: 178

- Introduction: 448

- Discussion: 1561

- Total (Abstract, Introduction, Materials & Methods, Results, Discussion, References and Figure Legends): 8221

Keywords: synaptic vesicle cycle - GABA - tetraspan vesicle membrane protein - synaptogyrin - synaptophysin - *Caenorhabditis elegans*

Acknowledgements: We thank Dr. Reinhard Windoffer (this institute) for helpful advice throughout the project and the *Caenorhabditis* Genetics Center (Minneapolis, MN), the Chisholm (San Diego, CA), Jorgensen (Salt Lake City, UT), Kennedy (Madison, WI) and Kaplan (Boston, MA) labs for worm strains. This work was supported by the German Research Council (LE 566/8; Graduate School "Entwicklungsabhängige und krankheitsinduzierte Modifikationen im Nervensystem") and the VolkswagenStiftung.

Abstract

The tetraspan membrane proteins of the synaptogyrin and synaptophysin type are abundant and evolutionary conserved synaptic vesicle membrane proteins whose functions are poorly defined. Their depletion does not interfere with proper neuronal development and basic neuronal function. In the search for their function we use the genetic model organism *C. elegans* in which, in contrast to vertebrates, the synaptogyrin but not the synaptophysin orthologue is predominant in neurons. Employing fluorescent reporter constructs we find that synaptogyrin is expressed in all GABAergic neurons and most, though not all other neurons. Subjecting animals either lacking or overexpressing synaptogyrin to the epileptogenic GABA antagonist pentylentetrazole reveals increased sensitivity in comparison to the wild type. Detailed analyses further uncover mildly altered motility, slightly reduced sensitivity to the acetylcholine esterase inhibitor aldicarb and decreased recruitment of synaptobrevin but not of RAB-3 to synapses. Furthermore, synthetic phenotypes are observed with mutants of the synaptic vesicle recycling machinery, notably with synaptotagmin, synaptojanin and endophilin rather than with mutants involved in clathrin-dependent endocytosis. Taken together, these observations assign a distinct modulatory and redundant neuronal function to synaptogyrin.

Introduction

Synaptophysins and synaptogyrins are major synaptic vesicle proteins (Hubner et al., 2002; Valtorta et al., 2004; Takamori et al., 2006; Burre and Volkandt, 2007). They are tyrosine-phosphorylated and are characterized by four membrane-spanning domains (Hubner et al., 2002; Evans and Cousin, 2005; Arthur and Stowell, 2007). Together with other vesicle membrane proteins that share the same transmembrane topology they are referred to as tetraspan vesicle membrane proteins (TVPs). They are encoded by multigene families in mammals and are evolutionary conserved throughout the animal kingdom (Hubner et al., 2002; Abraham et al., 2006). While synaptophysin is the major neuronal TVP in mammals, this property has been assigned to synaptogyrin (SNG-1) in *C. elegans* (Nonet, 1999; Hubner et al., 2002; Abraham et al., 2006; Ruvinsky et al., 2007). It has been demonstrated recently that murine synaptophysins

and synaptogyrins associate with each other both *in vitro* and *in vivo* (Felkl and Leube, 2008). Despite their abundance in synaptic vesicles and their evolutionary conservation, only very little is known about their function. It has been shown in mouse and *C. elegans* that they are completely dispensable for nervous system development and performance of basic neuronal functions (Eshkind and Leube, 1995; McMahon et al., 1996; Abraham et al., 2006), although they are tightly associated with components of the synaptic vesicle recycling machinery (cf. (Hubner et al., 2002)). Only very minor deficiencies have been reported to date in gene depletion experiments. Thus, a slight decrease of synaptobrevin expression, morphological changes of photoreceptors and mild alterations in learning and behavior were observed in synaptophysin knockout mice (McMahon et al., 1996; Spiwox-Becker et al., 2001; Schmitt et al., 2009). In TVP-deficient *C. elegans* an increase in clathrin-coated vesicles was noted (Abraham et al., 2006). Further analyses of synaptogyrin/synaptophysin double knockout mice revealed defects in synaptic plasticity (Janz et al., 1999).

Given the difficulty to assign neuronal functions to synaptophysins and synaptogyrins, we further exploited the suitability of the model organism *C. elegans* to perform large scale assays. We extend previous data by showing that synaptogyrin is the major neuronal TVP polypeptide which is expressed in all 26 GABAergic neurons and most though not all other neurons. Using the competitive GABA antagonist pentylentetrazole (PTZ) we find that the convulsive threshold of worms either lacking or overexpressing synaptogyrin is reduced in comparison to the wild type. Detailed analyses further reveal mild changes in motility, reduced synaptic recruitment of synaptobrevin and a slightly increased resistance to the acetylcholine esterase inhibitor aldicarb. Crossing synaptogyrin-deficient worms with worms mutant for other synaptic vesicle components further reveals synthetic phenotypes. Taken together, the data suggest that synaptogyrin either acts as a modulator of neurotransmission and/or is involved in an alternative synaptic vesicle pathway.

Material and Methods

Gene constructs

Transcriptional reporter construct *sng-1p::cfp* was prepared by first amplifying a 3,579 bp *Sall/BamHI*-flanked promoter fragment with amplimers 05-132 (5'-GGA GGA GTC GAC GTA GAT TCA ACC GAG CAT TC-3') and 05-133 (5'-GGA GGA GGA TCC GGG TCA GAG GTG TTC AGA TTC-3') from cosmid T08A9. This fragment was subsequently cloned into vector pVH10.10 carrying the CFP-encoding cDNA (Hutter, 2003). A vector containing *sng-1p::yfp* was described recently (Abraham et al., 2006).

To prepare hybrid gene *sng-1::yfp*, a 6,544 bp *BamHI/XmaI*-flanked fragment was amplified with oligonucleotides 00-18 (5'-CGG GAT CCG GGA TTA GTA CTT GTG AAT GAG-3') and 00-15 (5'-TCC CCC CGG GCA TAA CCA TAT CCT TCC GAC T-3') from cosmid T08A9 which was then inserted into pVH20.01 (Hutter, 2003).

For preparation of rescue construct *sng-1p::sng-1* a 553 bp *XmaI/NcoI*-flanked fragment was amplified with primers 06-117 (5'-CAT CCC GGG TAG TTT TTT AGC CAA AC-3') and 06-118 (5'-CCA CCA TGG GTT GAA AAT AAA ACT TGA AG-3') from cosmid T08A9 and cloned into the *sng-1::yfp*-containing vector.

The transcriptional reporter construct *ifb-2p::yfp* was prepared by amplifying the 1,994 bp *ifb-2* promoter fragment from genomic DNA as described (Husken et al., 2008) and inserting it into the *HindII/PstI* sites of the *yfp*-containing vector pVH20.01 (Hutter, 2003).

The GABAergic rescue construct *unc-25p::sng-1* was generated by first amplifying a *HindIII/BamHI*-flanked *unc-25* promoter fragment with amplimers 10-135 (5'-TTA AGC TTG TCG ACT TTA AAA AAA TAT TTT TTT TTT CAG AAA ATA AGA AAA GCC G-3') and 10-136 (5'-TGG ATC CGC GGC CGC TCT AGA TTT TGG CGG TGA ACT GAG C-3') from genomic DNA. The promoter was then inserted into *HindIII/BamHI*-digested pVH20.01. Additionally, a 1866 bp *NotI/BamHI*-fragment encompassing the entire coding region of the *sng-1* gene was amplified with amplimers 10-137 (5'-AAG CGG CCG CGG TAC CAT GGA GAA CGT GCG TGC TTA TG-3') and 10-138 (5'-TAG GAT CCG ATA TCT CTA GAT TAA GAT

ATC ATA ACC ATA TCC TTC CGA C-3') from genomic DNA and placed into the *unc-25p*-containing vector.

Worm strains and RNAi-mediated interference

Animals were cultured on NGM-agar plates by standard techniques. A complete list of strains used in this study is provided in Table 1.

For RNA-mediated interference NGM-agar plates containing 25 µg/ml carbenicillin (Roth) and 1 mM isopropyl-β-D-thiogalactopyranoside (Fermentas) were inoculated with 200 µl of an overnight HT115 culture containing dsRNAi-producing plasmids (empty vector L4440 (Fraser et al., 2000) and HGMP ID X-3F24 for *sng-1*). Plates were incubated at room temperature overnight before placing four L4 of RNAi-sensitive strain GR1373 *eri-1(mg366)IV* on each plate. The F1 progeny was analyzed after incubation at 20°C.

RT-PCR

Young adult worms grown on agar plates were washed with M9 medium (41 mM Na₂HPO₄, 25 mM KH₂PO₄, 10 mM NaCl, 20 mM NH₄Cl) and centrifuged. The resulting worm pellet was dissolved in 1 ml Trizol reagent (Invitrogen), frozen in liquid nitrogen and ground into a fine powder in a mortar. The RNA was subsequently extracted with phenol/chloroform/isoamyl alcohol (Applied Biosystems) and cleaned with the help of the RNeasy-Kit (Qiagen). 1 µg of purified total RNA was reverse transcribed with oligo-dT primer using the Transcriptor First Strand cDNA Synthesis Kit (Roche). The resulting cDNA was analyzed by semiquantitative PCR with the help of a LightCycler (Roche) using the LightCycler TaqMan Master Kit (Roche). Primer and TaqMan probes for synaptogyrin (forward primer 5'-TGG ATA CGG AGG AGA CTC AAC-3', reverse primer 5'-AGC ACC AGA TTG GTA TGA GGA-3', UPL#39) and GAPDH (forward primer 5'-CGA CCC TCA CTC GTC CAT-3', reverse primer 5'-CAA CAC GGT TCG AGT ATC CA-3', UPL#67) were obtained from the Universal Probe Library Assay

Design Center (Roche). Quantitative analyses were performed on two separately prepared cDNAs and were done in triplicate in each case. The results were analyzed using the RelQuant Software (Roche).

Microscopy

Young adult worms were taken from fresh plates for fluorescence microscopy. Fluorescence patterns were analyzed by confocal laser scanning microscopy using a Leica TCS SP5 (Bensheim, Germany). Worms were placed in a 20 μ l drop of M9 medium containing 1 mM sodium azide on slides with a thin 2% agarose pad. A cover slip was put on top. The duration of recording never exceeded 1 h. The resonance scanner mode was used and the pinhole area was set at 1. 100 - 300 stacks were produced per animal. Images were processed and adjusted in ImagePro Plus and further analyzed with the 3D-reconstruction program Amira. Animated sequences were converted into mpeg-1 format.

Motility of worms was recorded by time-lapse imaging of worms under the dissection microscope (Leica MZ16FA and Nikon SMZ1500) with either a CCD video camera (Sony) or a USB camera (IDS-Imaging Development Systems). The amplitudes of the sinusoidal movement were measured with the help of ImagePro Plus software (Media Cybernetics Inc.), ImageJ (NIH) and uEye (IDS-Imaging Development Systems).

The fluorescent pattern of dorsal nerve cords of young adult reporter strains (for details see Table 1) were recorded with the Zeiss Imager.M2 microscope. Images were subsequently processed with ImagePro Plus and analyzed with Igor Pro (Wavemetrics Incorporation) as described (Sieburth et al., 2005; Ch'ng et al., 2008, Vashlishan et al., 2008).

Pharmacological assays

To test the GABAergic system, worms were treated with the competitive GABA antagonist pentylentetrazole according to published protocols (Williams et al., 2004). In brief, 20 mg/ml

stock solutions were prepared by dissolving pentylenetetrazole in water, which was used for further dilutions. 400 μ l of the concentrated or diluted solutions were spread over 35 mm diameter Petri dishes with agar prepared in normal growth medium (NGM) that had been dried for 2-4 h at room temperature. After 1 h incubation at room temperature young adult animals that had been washed with M9 medium were added. 30 min later (incubation in complete darkness at room temperature) cramping was assessed by blinded visual inspection and documented by video recording.

To test the cholinergic system, a kinetic aldicarb assay was performed. To this end, the acetylcholine esterase inhibitor aldicarb (Supelco) was dissolved in acetone (100 mM stock solution) and diluted to 400 μ l/10 g agar to final concentrations of 0.5 mM and 1 mM. The solution was added to bacteria-free 3.5 cm NGM-agar plates. After a brief drying step young adult worms were placed on these plates and their motility was assessed at 30 min, 1 h, 2 h, 3 h, and 4 h after short nose touch with an eyebrow hair.

Pharyngeal pumping

Pharyngeal pumping assays were performed on young adults on agar plates in the absence of any drug. The frequency of pharyngeal pumping was determined by counting posterior bulb contractions for 1 min per animal. 10 animals were examined in each experiment and two independent experiments were performed for each genotype.

Statistics

Results are presented as mean \pm SEM. Experimental data were analyzed by Kolmogorow-Smirnow-Test (KS-Test), by paired Student's t-Test and by One-Way ANOVA Bonferroni's Multiple Comparison Test (rating of differences according to P-value: ***, $P < 0.001$; **, $P < 0.01$; *, $P < 0.05$).

Results

Loss as well as increase of synaptogyrin expression is associated with elevated pentylentetrazole sensitivity

To challenge the function of the GABAergic system in synaptogyrin mutant worms, outcrossed strain BJ14 *sng-1(ok234)* was treated with the competitive GABA antagonist pentylentetrazole (PTZ). As wild type controls N2 derivatives of strain BJ20 were used that had been obtained from the same outcross (Abraham et al., 2006). The mutant animals showed considerably increased sensitivity to PTZ. The cramping worms presented a walking stick-like body posture with the anterior part still remaining mobile (Fig. 1C; Movie 1). When the nose was touched with an eye brow hair, however, animals regained sinusoidal mobility. This was different to the synaptobrevin mutant *snb-1(md247)* which also cramped but reacted by increased spasms upon touch. Significant differences between *sng-1* mutants and wild type *wt* were already noticeable at 1 mg/ml PTZ and reached a plateau at 4 mg/ml (Figs. 1A, B). At concentrations between 4 mg/ml and 10 mg/ml PTZ ~60% of the *sng-1* mutants cramped, while wild type animals were not affected (Fig. 1B, C; Movies 1, 2). At higher PTZ concentrations an increasing number of wild type worms cramped (Fig. 1A). As expected, PTZ sensitivity could also be elicited by RNAi through bacterial feeding of *sng-1* dsRNA in an RNAi-sensitized genetic background, *eri-1(mg366)*, although at somewhat reduced efficiency (Fig. 2A).

To test the effect of synaptogyrin overexpression, a plasmid containing the synaptogyrin cDNA under *sng-1* promoter control (*sng-1p::sng-1*) was prepared. When we examined animals of strain BJ120 *kcEx19[sng-1p::sng-1, ifb-2p::yfp]* expressing this transgene together with a non-neuronal marker (Husken et al., 2008), slightly increased PTZ sensitivity was observed at 4 mg/ml and a significant increase in PTZ sensitivity was noted at 8 mg/ml in comparison to the wild type (Fig. 2B). At 8 mg/ml PTZ the number of cramping animals was similar to that observed for *sng-1* mutants.

To rescue the phenotype of synaptogyrin-deficient worms, the synaptogyrin gene construct *sng-1p::sng-1* was microinjected into the distal gonad of *sng-1* mutants together with the non-neuronal marker *ifb-2p::yfp*. Resulting transgenic worms of the rescued strain BJ103

kcEx12[sng-1p::sng-1, ifb-2p::yfp]; sng-1(ok234) were then subjected to PTZ assays. Intermediate PTZ concentrations were chosen at which the most pronounced phenotypes had been noted in the mutant worms (Fig. 1B). To make sure that the tested animals contained the rescue construct, only fluorescent animals were analyzed and the transgene was amplified by PCR after experimentation for further corroboration of *sng-1p::sng-1* expression. Fig. 3 shows that the achieved rescue was complete.

Quantitative RT-PCR analyses were performed to estimate the amount of mRNA expression in rescued *sng-1(r)* worms (BJ103) and *sng-1(+)* worms overexpressing *sng-1* (BJ120). While the amount of *sng-1* in wild type animals was 0.78 ± 0.09 (arbitrary units), it was 1.39 ± 0.34 in *sng-1(r)* and 3.43 ± 0.18 in *sng-1(+)*. The latter value is still a considerable underestimate of the degree of overexpression, since only 37% of animals carry the extrachromosomal array. As expected, no transcripts were detected in *sng-1* mutants.

Although it has been suggested that synaptogyrin is a pan-neuronal marker of synaptic specializations in *C. elegans* (e.g., (Nonet, 1999; Cinar et al., 2005; Ruvinsky et al., 2007)), precise localization with respect to the GABAergic system is still incomplete. Therefore, strain BJ60 *kcEx3[sng-1p::cfp]; oxIs12[lin-15(+), unc-47p::gfp], lin-15(n765ts)* was established by crossing *sng-1p::cfp*-containing worms of strain BJ31 with *unc-47p::gfp*-carrying strain EG1285, which produces GFP under the control of the vesicular GABA-transporter promoter (McIntire et al., 1997). The latter is synthesized in all 26 GABAergic neurons but not in other cells. The confocal double fluorescence images shown in Fig. 4 demonstrate that all of these neurons co-express CFP. Animations of the 3D-reconstructions further support this conclusion (Movies 3 and 4) and reveal, in addition, a *hitherto* unidentified 27th cell close to the posterior pharyngeal bulb that is positive for both markers. Although we did not unequivocally identify this cell, it is most likely another GABAergic neuron.

Syaptogyrin reporters are produced in most but not all neurons

Further inspection of *sng-1p::cfp*-induced fluorescence revealed that it is present in cells other than *unc-47p::gfp*-positive GABAergic neurons. Of note, a strong signal was seen for *sng-1p*-

driven CFP and YFP in anterior extensions, the nerve ring, the ventral nerve cord and dorsal nerve cord (Fig. 5A, top). In addition, multiple commissures could be identified. Further analyses revealed, however, that not all neurons are positive for *sng-1* expression. For example, amphids and phasmids were negative. Fig. 5Aa-A" and Movie 5 present comparisons of P_{sng-1}::YFP-mediated fluorescence and DiI, that was taken up into amphids ASK, ADL, ASI, AWB, ASH, and ASJ, demonstrating lack of co-localization. Similarly, phasmids PHA and PHB that were also labeled by DiI did not show *sng-1* transcription (Fig. 5Ap-A"p; Movie 6). Furthermore, we did not find evidence for synaptogyrin production in either of the other amphid neurons. Instead, the cephalic neurons CEPDR/L and CEPVR/L were tentatively positive (Fig. 5Aa). In addition, the glial-like sheath cells CEPshDR/L and CEPshVR/L, which are associated with the dendritic processes of the CEP neurons and partially enwrap the nerve ring (Shaham, 2006), were also likely labeled (Fig. 5A). Examination of SNG-1::YFP fusions (e.g., Fig. 5B) showed an identical distribution pattern to that observed for *sng-1p*::YFP. As expected, SNG-1::YFP, however, presented a multipunctate fluorescence typical for synaptic terminals. Next, embryos were analysed to further examine the relationship between the manifestation of the neuronal phenotype and synaptogyrin. At the onset of neurulation (1.25-fold stage), the first neuronal precursor cells were positive for both reporters (Fig. 6). The signal subsequently increased in the developing nervous system.

Alterations in synaptogyrin expression induce mild changes in aldicarb resistance and in motility

The severe PTZ phenotype of worms with altered synaptogyrin expression and the broad neuronal distribution of synaptogyrin led us to re-investigate the sensitivity of mutant worms to the acetylcholine esterase inhibitor aldicarb. We had previously only examined triple-mutant strain BJ21 that, in addition to the *sng-1(ok234)* allele, carries mutant alleles *sph-1(ox278)* and *scm-1(hd30)* encoding two other tetraspan vesicle membrane proteins (Abraham et al., 2006). Since we had not been able to detect any defect using a simple aldicarb assay, we now refined the assay for the *sng-1(ok234)* single mutant by monitoring aldicarb sensitivity over time. Thus, a slight and statistically significant increase in aldicarb resistance (*ric*) was observed at 0.5 mM aldicarb, but not at higher aldicarb concentrations (Fig. 7A, B). Remarkably, worms

overexpressing synaptogyrin (strain BJ120) were even more *ric* (*sng-1*(+)) in Fig. 7A, B).

Given that locomotion is regulated by both GABAergic and cholinergic neurons, motility was digitally analyzed. Locomotion of worms on agar plates was recorded by video microscopy. Examination of the resulting images revealed highly significant differences in the amplitude of the sinusoidal motility of wild type (*wt*) and either *sng-1* mutant or synaptogyrin-overexpressing *sng-1*(+) worms (Fig. 7C). The change in the amplitude could be rescued by expressing SNG-1 either under the control of its own promoter (*sng-1*(r)); Fig. 7C, D) or using the GABAergic promoter *unc-25p* (*sng-1*(gr1) strain BJ180, *sng-1*(gr2) strain BJ181, *sng-1*(gr3) strain BJ182 and *sng-1*(gr4) strain BJ190 in Fig. 7D).

Synaptobrevin is less efficiently recruited to synaptic sites in synaptogyrin mutants

In a previous study the density of synapses using SNB-1::GFP as a marker in triple-mutant worms lacking not only SNG-1 but also the related tetraspanins SPH-1 and SCM-1 was found to be unaltered (Abraham et al., 2006). In search for more subtle and yet unidentified differences further reporter strains were examined in detail. In accordance with the previous observations we found that loss of SNG-1 does not alter the density of synapses either in GABAergic reporter strains carrying allele *juIs1*[*unc-25p::snb-1::gfp*] or cholinergic reporter strains carrying allele *nuIs152*[*unc-129p::gfp::snb-1, ttx-3p::mrfp*] (Table 2). But the width of the GABAergic synaptic puncta is significantly increased (Table 2) coincident with an increase in cord fluorescence ($0.74 \pm 0.25 \mu\text{m}$ for *juIs1/wt* versus $2.18 \pm 0.45 \mu\text{m}$ for *juIs1/sng-1*; $P=0.02$ by KS-Test). Both width and cord fluorescence phenotypes could be rescued by expressing *sng-1* under the control of the GABAergic promoter *unc-25p* (strain BJ197). The rescued width ($1.11 \pm 0.02 \mu\text{m}$) was not different from the wild type ($P=0.6$ by KS-Test), whereas the cord fluorescence (0.03 ± 0.01) was significantly overrescued ($P=0.001$ by KS-Test). Furthermore, comparing worms carrying the cholinergic reporter allele *nuIs152* a slight but significant increase of synaptic width was seen in *sng-1* mutants in comparison to wild type (Table 2) but no change in cord fluorescence (*nuIs152/wt* 1.72 ± 0.47 versus *nuIs152/sng-1* 1.08 ± 0.29 ; $P=0.3$ by KS-Test). Notably, the observed changes in the GABAergic and cholinergic nervous system are specific for

SNB-1, since RAB-3 (reporter *nuIs168[unc-129p::venus::rab-3, myo-2p::nls::yfp]*), another synaptic vesicle marker, was not altered in *sng-1* mutants (Table 2). Finally, the postsynaptic side was examined using the GABA-receptor UNC-49 tagged with GFP (allele *oxIs22[myo-3p::unc-49::gfp]*). No changes in density and width were detected (Table 2). This is also in accordance with the presynaptic localization of SNG-1 reporters co-distributing with synaptotagmin (Zhang and Nonet, 2001).

Synthetic phenotype of synaptogyrin mutation with mutations affecting genes that encode synaptic vesicle machinery components

To examine the function of synaptogyrin in relation to other components of the synaptic vesicle cycle, a screen for synthetic phenotypes was performed. To this end, EG3008 *sng-1(ok234)*, *oxIs12[lin-15(+), unc-47p::gfp]*, *lin-15(n765ts)* and *sng-1* mutant strain BJ14 were each crossed with strains containing mutations affecting presynaptic neurotransmission including components of the exo-/ endocytotic machinery and enzymes of lipid metabolism (Fig. 8). Most of the latter animals were barely able to move. Yet, some of the double mutants appeared to be even less motile. As a result, these double mutant worms could not move through the surrounding food source at all anymore and replication was considerably reduced. 4 days after placing L4 larvae on a bacterial lawn the food source was almost unused in some of the double mutants differing considerably from the respective single mutants. Of the genes tested, such synthetic phenotypes were observed for synaptotagmin (alleles *snt-1(md290)*, *snt-1(ad596)*, *snt-1(n2665)*), endophilin (alleles *unc-57(ok319)*, *unc-57(e406)*) and synaptojanin (allele *unc-26(m2)*) but not for mutant alleles of *fat-3*, *unc-1*, *unc-24*, *snb-1*, *unc-64*, *chc-1*, and *dyn-1* (Fig. 8C and data not shown). Given the very pronounced neuronal deficiencies it was quite difficult to find reliable assays for the comparison of neuronal functions of single and double mutants. Based on the presence of SNG-1 reporters in the modulatory pharyngeal neurons M3 and M4 (Fig. 4B), pharyngeal pumping assays were performed that could be easily carried out on the highly immotile worms and appeared to be suitable. They fully confirmed the above synthetic phenotypes (Fig. 8A). To further exclude an effect of the additional *oxIs12[lin-15(+), unc-47p::gfp]* alleles, which are present in the control strain and are *ric* in aldicarb assays (data not shown), the phenotypic

double-mutants were also tested in a background lacking these transgenes (Fig. 8B). The same phenotypes in food consumption and pharyngeal pumping were observed as found for *oxIs12*-containing strains (Figs. 8A-C).

Discussion

Elucidation of the contribution of the related synaptogyryns and synaptophysins to the synaptic vesicle cycle has turned out to be much more difficult than originally anticipated and is still far from complete. This difficulty is quite surprising considering the abundance of these polypeptides in synaptic vesicles (Takamori et al., 2006; Burre and Volkhardt, 2007), their tight association with components of the synaptic vesicle recycling machinery (e.g., (Edelmann et al., 1995; Daly et al., 2000; Felkl and Leube, 2008)) and with synaptic vesicle membrane transporters (e.g., (Siebert et al., 1994; Galli et al., 1996; Egana et al., 2009) as well as their evolutionary conservation (Hubner et al., 2002; Abraham et al., 2006). The presence of synaptogyryns and synaptophysins in the same complexes (Felkl and Leube, 2008), their complex species-specific neuronal expression patterns (e.g., (Stenius et al., 1995; Hubner et al., 2002; Belizaire et al., 2004; Abraham et al., 2006)) and their synthetic phenotypes in knockout mice (Janz et al., 1999) further suggest that they share functions and are, at least in part, exchangeable. The nematode synaptogyryn may therefore perform functions that are assigned to synaptophysin in vertebrates. This conclusion stems from the expression patterns observed with reporter fusions demonstrating synthesis of synaptogyryn in synapses of most neurons from the earliest time onward whereas the synaptophysin ortholog SPH-1 is, for the most part, absent in neurons (this study and (Nonet, 1999; Zhao and Nonet, 2001; Hubner et al., 2002; Abraham et al., 2006)). Especially in the case of synaptogyryn we are quite confident that the reporters reflect the synthesis from the endogenous gene: The promoter fragment that was used in the current study encompassed most of the upstream intergenic region and comparison of the overall distribution patterns of this transcriptional fusion with that of a translational reporter containing another 1074 bp of the upstream region and all introns revealed no differences. In addition, a rescue construct derived from the translational fusion worked well in reversing the mutant phenotype. Our data are also in full agreement with previous observations (Nonet, 1999; Hubner et al., 2002;

Abraham et al., 2006). Although synaptogyrin is undoubtedly a valuable neuronal marker in *C. elegans*, our current data also show that specific neurons, i.e., sensory amphids and phasmids, are negative for synaptogyrin. Some of these cells may produce other TVPs such as the secretory carrier-associated membrane protein (SCAMP) ortholog SCM-1 (Abraham et al., 2006). It will be interesting to find out, whether these major sensory neurons differ in their handling and usage of synaptic vesicles. Furthermore, we provide evidence that synaptogyrin production is not an exclusive property of neurons in *C. elegans* but occurs also in other cells, most notably the sheath cells surrounding the dendritic endings of CEP.

The discrepancy between lack of apparent function on one hand and the evolutionary conservation and abundance on the other hand can only in part be due to isotype redundancy, since double knockout mice and completely TVP-deficient *C. elegans* still present rather minor phenotypic alterations (Janz et al., 1999; Abraham et al., 2006). It is therefore likely, that redundancy in the form of non-related pathways is also of relevance and secures synaptic vesicle function. Thus, we sought to challenge neurotransmission in synaptogyrin mutant animals by pharmacological interference and further genetic manipulation. Using the epileptogenic pro-convulsive drug PTZ we succeeded in identifying a distinct neuronal phenotype in worms lacking or overexpressing synaptogyrin. The increased cramping response could be fully rescued with a synaptogyrin gene construct that is expressed in most neurons including all GABAergic neurons. Remarkably, exclusive GABAergic rescue of SNG-1 was sufficient to reconstitute normal motility as assessed by amplitude measurements. GABAergic neurons are particularly rich in synaptic vesicles and may therefore be especially susceptible to minor changes in synaptic vesicle recycling efficiency. In support, kindling experiments in rat led to an increase in the synaptophysin-synaptobrevin complex, which was interpreted as a way to adjust the reserve pool to an increased demand for synaptic vesicle recycling (Hinz et al., 2001). We suggest that the lack of the corresponding complex in *C. elegans* leads to the compromised response to PTZ in synaptogyrin-deficient worms.

The modulatory role of synaptogyrin is not restricted to the GABAergic system, however, since we had previously also detected structural changes in cholinergic synapses (Abraham et al., 2006) and now find significant, though minor changes in aldicarb sensitivity and in synaptic width of cholinergic neurons. The lack of alterations in osmotic avoidance, chemotaxis and

thermotaxis (Abraham et al., 2006) can be explained by the absence of synaptogyrin in the responsible amphids and phasmids. Our data now show that modulation of the synaptic vesicle cycle is tightly controlled by the specific amount of synaptogyrin present, since both decrease and increase of synaptogyrin resulted in a similarly altered sensitivity to PTZ and aldicarb and similarly altered locomotion. This apparent paradox may be explained by synaptogyrins' modulatory function as a platform for components of the synaptic vesicle recycling machinery (Felkl and Leube, 2008). Thus, absence of synaptogyrin compromises proper positioning of these components whereas overexpression retains the same components and thus reduces their availability. In line, synaptobrevin mutants display a similar, though more pronounced PTZ and aldicarb phenotype (Nonet et al., 1998; Williams et al., 2004). The different cramping behavior in this instance may be explained by the interference with the fusion machinery that is still intact in the synaptogyrin mutants. Furthermore, previous experiments have shown that overexpression of synaptophysin and synaptogyrin 1-3 interfere with calcium-dependent exocytosis of human growth hormone from neuroendocrine PC12 cells (Sugita et al., 1999). Similarly, injection of carboxyterminal synaptophysin peptides that prevent proper synaptophysin-dynamin interaction decreased transmitter release from the squid giant synapse during high-frequency stimulation (Daly et al., 2000). Also, elevated SCAMP1 synthesis led to a partial inhibition of transferrin endocytosis in COS cells that was almost completely abrogated by a deletion mutant lacking the aminoterminal NPF repeats which mediate clathrin-dependent endocytosis by binding EH-domain proteins (Fernandez-Chacon et al., 2000).

The observed synthetic phenotypes of synaptogyrin mutants together with mutants of either synaptojanin, endophilin or synaptotagmin are compatible with a function of synaptogyrin in clathrin-independent endocytosis, since synaptojanin, endophilin and synaptotagmin have all been implicated in this pathway (e.g., (Song and Zinsmaier, 2003; Jung and Haucke, 2007; Shupliakov, 2009)). This notion is in agreement with the previously observed compensatory up-regulation of clathrin-coated vesicles in synapses injected with peptides that disrupt the interaction between synaptophysin and dynamin (Daly et al., 2000). Furthermore, it has been shown that synaptobrevin, which binds tightly to synaptophysin, is involved in a clathrin-independent fast endocytic pathway (Deak et al., 2004) that may correspond to the "kiss and run" mode (Jung and Haucke, 2007; Smith et al., 2008). Consistent with these findings, we did not

detect synthetic phenotypes between synaptogyrin mutation and mutation of synaptobrevin. Similarly, mutation of another known binding partner of synaptophysin, dynamin, did also not present a synthetic phenotype with synaptogyrin in the current study. Direct interaction between synaptogyrin and either synaptobrevin or dynamin, however, still needs to be shown in *C. elegans*. Yet, the observation that the distribution of SNB-1 but not of other synaptic vesicle proteins such as RAB-3 is altered in the absence of SNG-1 can be taken as an indication for their physical interaction. Although the molecular details of this alternative pathway need to be elucidated, it appears that synaptogyrin/synaptophysin are of particular importance for recycling of vesicular transporters and their function, since (i) direct association has been reported for VACHT with the synaptobrevin/synaptophysin complex (Sandoval et al., 2006) and the dopamine transporter with synaptogyrin (Egana et al., 2009), (ii) synaptophysin is associated with subunits of the vacuolar ATPase (Siebert et al., 1994; Galli et al., 1996), and (iii) synaptophysin interacts with adaptor proteins (Horikawa et al., 2002) which affect, for example, VGAT targeting to synaptic vesicles (Nakatsu et al., 2004). Synaptophysins' function may be to stabilize the vesicle so that a certain amount of neurotransmitter can be released. Such a facilitatory role may be accomplished by providing a platform that favors multiple protein-protein interactions (Felkl and Leube, 2008).

In analogy, the major consequence of synaptogyrin loss in *C. elegans* is reduced neurotransmitter in the synaptic cleft. In the case of the GABAergic system, increased sensitivity to the competitive GABA receptor antagonist PTZ was therefore noted. It also explains the altered motility, because preferential reduction of GABAergic inhibition of muscle contraction in the presence of mostly normal cholinergic muscle stimulation leads to increased muscle tone and, hence, a reduction in amplitude. In addition, reduced neurotransmitter secretion is likely responsible for the feeding and pharyngeal pumping phenotypes, since the synaptogyrin-positive pharyngeal neurons M3 and M4 (Fig. 4B) affect feeding behaviour and pharynx relaxation (Avery and Thomas, 1997; Dent et al., 1997). Finally, slightly reduced acetylcholine secretion is the reason for the rather weak aldicarb phenotype.

The assignment of a non-essential role to synaptogyrin/synaptophysin does not preclude their relevance to human diseases. Especially in the case of psychiatric disorders and neurodegeneration they develop over long periods of time. Thus, minor alterations in synaptic

vesicle recycling caused by synaptophysin/synaptogyrin mutation or modification may compromise synaptic efficiency and thereby contribute to slow and long-term pathogenesis (eg, Mallozzi et al., 2009). Therefore, genetic links between synaptogyrin mutation and schizophrenia (Verma et al., 2004; Cheng and Chen, 2007; Iatropoulos et al., 2009) and the suggested links between synaptophysin alterations and dementia (Heffernan et al., 1998; Tran et al., 2003) merit further investigation.

Legends to figures

Figure 1. Synaptogyrin-deficient worms are hypersensitive to the GABA antagonist PTZ. **A**, The histogram depicts the percentage of cramped animals after a 30 min treatment with either 1 mg/ml PTZ (left) or 20 mg/ml PTZ (right). Note the increased sensitivity of *sng-1* mutant strain BJ14 (n=113) in comparison to the wild type (*wt*) strain BJ20 (n=211). As a positive control, synaptobrevin mutant (*snb-1*, (strain NM467; n=287) was used. Data were compared by One-Way ANOVA Bonferroni's Multiple Comparison Test. **B**, Graph, showing that the differences between *wt* and *sng-1* are most pronounced at intermediate PTZ concentrations (*wt*: n=124 at 4 mg, n=138 at 6 mg, and n=117 at 8 mg, n=128 at 10 mg; *sng-1*: n=51 at 4 mg, n=60 at 6 mg, and n=57 at 8 mg, n=57 at 10 mg; and *snb-1*: n=154 at 4 mg, n=143 at 6 mg, n=140 at 8 mg, and n=121 at 10 mg). All experiments were blinded and done in triplicate. Comparisons were analyzed by paired Student's t-Test (P<0.001 for all concentrations). **C**, The micrographs were taken from video recordings (Movies 1, 2) and depict representative worms of strains BJ20 (*wt*), BJ14 (*sng-1*) and NM467 (*snb-1*) in the presence of 6 mg/ml PTZ. Note the cane-like distortion of *sng-1* mutants. Bars, 100 μ m.

Figure 2. Decrease and increase of synaptogyrin are both associated with elevated PTZ sensitivity. **A**, The histogram shows results of representative blinded experiments investigating PTZ sensitivity of RNAi-sensitive strain GR1373 *eri-1(mg366)* after feeding with bacteria producing *sng-1* RNAi (n=9 at 6 mg/ml; n=5 at 8 mg/ml; n=9 at 10 mg/ml) or bacteria containing an empty vector (*wt*; n=10 at 6 mg/ml; n=10 at 8 mg/ml; n=9 at 10 mg/ml). *sng-1*

mutant strain BJ67 was used as a positive control (n=9 at 6 mg/ml; n=8 at 8 mg/ml; n=5 at 10 mg/ml). **B**, The histogram presents results of blinded experiments performed independently in triplicate. Differences were analyzed by One-Way ANOVA Bonferroni's Multiple Comparison Test. Shown are the percentages of cramped worms in the presence of either 4 mg/ml (left) or 8 mg/ml PTZ (right). The worms examined were either wild type (*wt* [BJ20]; n=140 at 4 mg/ml and n=152 at 8 mg/ml), synaptogyrin-deficient (*sng-1* [BJ14]; n=120 at 4 mg/ml and n=122 at 8 mg/ml), or contained additional *sng-1* copies (*sng-1(+)* [BJ120]; n=114 at 4 mg/ml and n=100 at 8 mg/ml).

Figure 3. The PTZ phenotype of synaptogyrin mutants can be fully rescued. The histogram depicts the percentage of cramped worms in the presence of either 4 mg/ml PTZ (left) or 8 mg/ml PTZ (right) observed in three independent and blinded experiments. Worms used were either wild type (*wt*, BJ20; n=148 for 4 mg/ml and n=134 for 8 mg/ml), *sng-1* mutant (BJ14; n=134 for 4 mg/ml and n=126 for 8 mg/ml), or *sng-1* mutants with a microinjected *sng-1* gene construct (*sng-1(r)* (BJ103; n=146 for 4 mg/ml and n=138 for 8 mg/ml). Note the reversion of the mutant phenotype after microinjection of the *sng-1* gene into the mutant (analysis by One-Way ANOVA Bonferroni's Multiple Comparison Test).

Figure 4. Synaptogyrin transcription occurs in all GABAergic neurons of adult worms. The projected confocal fluorescence image stacks (reconstructed survey view in **A**; anterior and posterior ends in **B** [corresponding Movies 3 and 4]) depict strain BJ60 *kcEx3[sng-1p::cfp]; oxIs12[lin-15(+), unc-47p::gfp], lin-15(n765ts)X* synthesizing *sng-1p::CFP* (blue) together with *unc-47p::GFP* (red), which specifically labels all 26 GABAergic neurons (numbered arrowheads) producing the vesicular GABA-transporter. Both reporters are co-expressed in all GABAergic neurons including also RMER which cannot be identified in the projected images but is visible in Movie 3. To avoid unspecific bleed-through between the different channels, a narrow detection window was chosen resulting in weak fluorescence signals in some of the commissures all of which were positive, however, upon detailed examination (commissures are demarcated as a-p in **A**). The red fluorescence observed in intestinal cells is caused by

autofluorescence. The higher magnification images in **B** (corresponding Movies 3, 4) reveal that the *sng-1p::CFP* labeling is much more extensive than that of *unc-47p::GFP*. Arrows indicate, for example, lateral neuronal processes and neurons MI, M4 and M3R/L that are only positive for *sng-1p::CFP*. Cross hairs in A for orientation: a, anterior; p, posterior; d, dorsal; v, ventral; l, left; r, right.

Figure 5. Synaptogyrin is expressed in most neurons but is absent in amphids and phasmids and can be detected in non-neuronal glial-like sheath cells in adult worms. **A**, The reconstructed confocal fluorescence micrographs show the distribution of Psng-1:YFP in the anterior part (Aa) and posterior part (Ap) of a worm of strain BJ23 *kcEx2[sng-1p::yfp]* in comparison to DiI-labeled amphids ASK, ADL, ASI, AWB, ASH, and ASJ (A'a) and phasmids PHA and PHB (A'p). The merged images in A'a and A'p depict *sng-1p::YFP* fluorescence in false blue color and DiI fluorescence in red demonstrating complete absence of co-localization (see also Movies 5, 6). Instead, the cephalic neurons CEPDR/L and CEPVR/L and amphid-associated sheath cells CEPshDR/L, CEPshVR/L were tentatively positive (the respective cells of the left body site are labeled by a blue square and blue sphere in Aa). 1 points to the characteristic ensheathment of a cephalic neuronal dendritic process by a sheath cell. Several other neurons that could be tentatively identified in the anterior part are MI, M4, I4, AVL, AIY, RIS, I5, M3R/L and in the posterior part DVA, AS11, ALNR/L, DVC, DVB, PQR, DA9 (characteristic axonal process denoted by arrowhead), VD13, DD6, VD12. Of these, AVL, RIS, VD13, DD6 and VD12 are GABAergic based on the colocalization with the *unc-47p::GFP* reporter (Fig. 4A). In addition, IL neurons were tentatively identified in the anterior (IL*). **B**, The projected confocal images depict the fluorescence of the translational fusion SNG-1::YFP (strain VH180 (Abraham et al., 2006)) in relation to DiI-labeled amphids and phasmids demonstrating the same lack of overlap as in A. 2 points to the position of neurons MI and M4, 3 to neuron M3 (compare with A and Fig. 1 B). * Denotes fluorescent bacteria adhering to the cuticle. Orientation: left, anterior; right, posterior; top, dorsal; bottom, ventral. Bars, 20 μ m.

Figure 6. Synaptogyrin reporter constructs are expressed in developing neurons. The projected confocal fluorescence image stacks depict fluorescence of transcriptional reporters in strain BJ23 *kcEx2[sng-1p::yfp]* at left and translational reporters in strain BJ107 *kcEx8[sng-1::yfp]* at right during different embryonic stages as indicated. Embryos are oriented with their anterior to the left and dorsal to the top. Red lines mark embryo borders as determined from phase contrast images. The expression of *sng-1p::YFP* is closely associated with the development of the nervous system being absent in the gastrula stage with first fluorescence in neuronal precursor cells (arrows) and newly-formed neurons (yellow arrowheads) in the anterior part during the 1.5-fold stage. In addition, it is also detected transiently in cells in the posterior body at the 1.25-fold and 1.5-fold stage. Note the similar cellular localization of the punctate SNG-1::YFP fluorescence that is most pronounced in the 3.0-fold stage. Size bars, 10 μ m.

Figure 7. Depletion and overexpression of synaptogyrin both confer increased aldicarb resistance and altered locomotion. **A, B** The graphs show results of four independent experiments in which worms were treated with 0.5 mM and 1.0 mM aldicarb, respectively. Motility was evaluated visually after a short touch with an eye brow hair at regular intervals for 4.5 h. Using the paired Student's t-Test, the values measured for *sng-1* mutant BJ14 (n=113 at 0.5 mM aldicarb; n=119 at 1.0 mM aldicarb) were significantly different from the wild type (*wt*) BJ20 (n=115 at 0.5 mM aldicarb; n=114 at 1.0 mM aldicarb) only when measurements at all time points were compared at 0.5 mM aldicarb (P=0.003) but not at 1 mM aldicarb (P=0.07). In contrast, significant differences were found for *sng-1(+)* strain BJ120 overexpressing SNG-1 (n=87 at 0.5 mM aldicarb; n=79 at 1.0 mM aldicarb) vs. *wt* at both aldicarb concentrations (P=0.003 at 0.5 mM; P=0.01 at 1 mM). **C**, Mobility of worms was video recorded and the amplitude of the sinusoidal movement was measured. Using One-Way ANOVA Bonferroni's Multiple Comparison Test, both *sng-1* (n=62) and *sng-1(+)* (n=62) presented significantly reduced amplitudes in comparison to wild type *wt* (n=62;). **D**, The histogram depicts amplitude measurements, that were obtained from two independent experiments in each instance, recording *sng-1* mutant worms (BJ14; n=204) in comparison to wild type (*wt* [BJ20]; n=203; P<0.001 with One-Way ANOVA Bonferroni's Multiple Comparison Test) and mutant strains rescued by GABAergic replenishment of SNG-1 (*sng-1*(gr1) [BJ103; n=130]; *sng-1*(gr2) [BJ180; n=199];

sng-1(gr2) [BJ181; n=96]; *sng-1(gr3)* [BJ182; N=181]; *sng-1(gr4)* [BJ190; n=31]), all of which were significantly different from the mutant but not different from the pan-neuronal *sng-1(r)* rescue strain (not shown). This demonstrates complete reconstitution of motility by GABAergic rescue.

Figure 8. Breeding of *sng-1* mutants with other mutants of synaptic vesicle proteins reveals synthetic phenotypes. **A**, The histogram depicts the results of pharyngeal pumping assays. Pumping rates were determined for 10 animals in each assay, all of which were performed in duplicate. Details of the strains used are given in **D** and Table 1. By One-Way ANOVA Bonferroni's Multiple Comparison Test. **B**, This histogram also summarizes results of pharyngeal pumping assays (n=20 for each column; two independent experiments) using another series of single and double mutants lacking the *sng-1*-linked marker *oxIs12* (for details see **D** and Table 1). **C**, Pictures show bacterial lawns with worms of different strains as indicated (for genotypes see **C**). 15 μ l of an overnight HB101 culture were put on NGM-agar plates. After a 24 h incubation at 37°C, a single L4 was placed in the middle of the bacterial lawn. Pictures were taken after 4 days at 20°C. Note the differences in remaining bacteria between single- and double-mutant worms. **D**, Details on strains used for the experiments shown in A-C.

Legends to movies

Movie 1. Behavior of *sng-1(ok234)* (BJ14) at a PTZ concentration of 6 mg/ml (corresponding Fig. 1C).

Movie 2. Behavior of wild type (BJ20) at a PTZ concentration of 6 mg/ml (corresponding Fig. 1C).

Movie 3. Animation of *sng-1p::CFP* and *unc-47p::GFP* fluorescence images recorded by

confocal laser scanning microscopy in the anterior end of a worm of strain BJ60 *kcEx3[sng-1p::cfp]; oxIs12[lin-15(+), unc-47p::gfp], lin-15(n765ts)X* (corresponding Figure 4B anterior).

Movie 4. Animation of *sng-1p::CFP* and *unc-47p::GFP* fluorescence images recorded by confocal laser scanning microscopy in the posterior end of a worm of strain BJ60 *kcEx3[sng-1p::cfp]; oxIs12[lin-15(+), unc-47p::gfp], lin-15(n765ts)X* (corresponding Fig. 4B posterior).

Movie 5. Animation of fluorescence distribution observed for *sng-1p::YFP* and DiI in anterior part of a worm of strain BJ23 *kcEx2[sng-1p::yfp]* using confocal laser scanning microscopy (see corresponding Fig. 5Aa, A'a, A"a).

Movie 6. Animation of fluorescence distribution observed for *sng-1p::YFP* and DiI in posterior part of a worm of strain BJ23 *kcEx2[sng-1p::yfp]* using confocal laser scanning microscopy (see corresponding Fig. 5Ap, A'p, A"p).

Table 1. Complete list of strains used in this study.

Table 2. Measurements of synaptic density and synaptic width using different fluorescent markers. Differences between wild type (*wt*) and *sng-1* mutant strains (*sng-1*) were determined by KS-Test.

References

- Abraham C, Hutter H, Palfreyman MT, Spatkowski G, Weimer RM, Windoffer R, Jorgensen EM, Leube RE (2006) Synaptic tetraspan vesicle membrane proteins are conserved but not needed for synaptogenesis and neuronal function in *Caenorhabditis elegans*. *Proc Natl Acad Sci U S A* 103:8227-8232.
- Arthur CP, Stowell MH (2007) Structure of synaptophysin: a hexameric MARVEL-domain channel protein. *Structure* 15:707-714.
- Avery L, Thomas JH (1997) Feeding and defecation. In: *C. elegans II* (Riddle DL, Blumenthal T, Meyer BJ, Priess JR, eds), pp 679-716. Cold Spring Harbor: Cold Spring Harbor Laboratory Press.
- Belizaire R, Komanduri C, Wooten K, Chen M, Thaller C, Janz R (2004) Characterization of synaptogyrin 3 as a new synaptic vesicle protein. *J Comp Neurol* 470:266-281.
- Burre J, Volkandt W (2007) The synaptic vesicle proteome. *J Neurochem* 101:1448-1462.
- Cheng MC, Chen CH (2007) Identification of rare mutations of synaptogyrin 1 gene in patients with schizophrenia. *J Psychiatr Res* 41:1027-1031.
- Ch'ng Q, Sieburth D, Kaplan JM (2008) Profiling synaptic proteins identifies regulators of insulin secretion and lifespan. *PLoS Genet* 4:e1000283.
- Cinar H, Keles S, Jin Y (2005) Expression profiling of GABAergic motor neurons in *Caenorhabditis elegans*. *Curr Biol* 15:340-346.
- Daly C, Sugimori M, Moreira JE, Ziff EB, Llinas R (2000) Synaptophysin regulates clathrin-independent endocytosis of synaptic vesicles. *Proc Natl Acad Sci U S A* 97:6120-6125.
- Deak F, Schoch S, Liu X, Sudhof TC, Kavalali ET (2004) Synaptobrevin is essential for fast synaptic-vesicle endocytosis. *Nat Cell Biol* 6:1102-1108.
- Dent JA, Davis MW, Avery L (1997) *avr-15* encodes a chloride channel subunit that mediates inhibitory glutamatergic neurotransmission and ivermectin sensitivity in *Caenorhabditis elegans*. *EMBO J* 16:5867-5879.
- Edelmann L, Hanson PI, Chapman ER, Jahn R (1995) Synaptobrevin binding to synaptophysin: a potential mechanism for controlling the exocytotic fusion machine. *EMBO J* 14:224-231.
- Egana LA, Cuevas RA, Baust TB, Parra LA, Leak RK, Hochendoner S, Pena K, Quiroz M, Hong WC, Dorostkar MM, Janz R, Sitte HH, Torres GE (2009) Physical and functional interaction between the dopamine transporter and the synaptic vesicle protein synaptogyrin-3. *J Neurosci* 29:4592-4604.
- Eshkind LG, Leube RE (1995) Mice lacking synaptophysin reproduce and form typical synaptic vesicles. *Cell Tissue Res* 282:423-433.
- Evans GJ, Cousin MA (2005) Tyrosine phosphorylation of synaptophysin in synaptic vesicle recycling. *Biochem Soc Trans* 33:1350-1353.
- Felkl M, Leube RE (2008) Interaction assays in yeast and cultured cells confirm known and identify novel partners of the synaptic vesicle protein synaptophysin. *Neuroscience* 156:344-352.
- Fernandez-Chacon R, Achiriloaie M, Janz R, Albanesi JP, Sudhof TC (2000) SCAMP1 function in endocytosis. *J Biol Chem* 275:12752-12756.
- Galli T, McPherson PS, De Camilli P (1996) The V0 sector of the V-ATPase, synaptobrevin, and synaptophysin are associated on synaptic vesicles in a Triton X-100-resistant, freeze-thawing sensitive, complex. *J Biol Chem* 271:2193-2198.

- Heffernan JM, Eastwood SL, Nagy Z, Sanders MW, McDonald B, Harrison PJ (1998) Temporal cortex synaptophysin mRNA is reduced in Alzheimer's disease and is negatively correlated with the severity of dementia. *Exp Neurol* 150:235-239.
- Hinz B, Becher A, Mitter D, Schulze K, Heinemann U, Draguhn A, Ahnert-Hilger G (2001) Activity-dependent changes of the presynaptic synaptophysin-synaptobrevin complex in adult rat brain. *Eur J Cell Biol* 80:615-619.
- Horikawa HP, Kneussel M, El Far O, Betz H (2002) Interaction of synaptophysin with the AP-1 adaptor protein gamma-adaptin. *Mol Cell Neurosci* 21:454-462.
- Hubner K, Windoffer R, Hutter H, Leube RE (2002) Tetraspan vesicle membrane proteins: synthesis, subcellular localization, and functional properties. *Int Rev Cytol* 214:103-159.
- Husken K, Wiesenfahrt T, Abraham C, Windoffer R, Bossinger O, Leube RE (2008) Maintenance of the intestinal tube in *Caenorhabditis elegans*: the role of the intermediate filament protein IFC-2. *Differentiation* 76:881-896.
- Hutter H (2003) Extracellular cues and pioneers act together to guide axons in the ventral cord of *C. elegans*. *Development* 130:5307-5318.
- Iatropoulos P, Gardella R, Valsecchi P, Magri C, Ratti C, Podavini D, Rossi G, Gennarelli M, Sacchetti E, Barlati S (2009) Association study and mutational screening of SYNGR1 as a candidate susceptibility gene for schizophrenia. *Psychiatr Genet* 19:237-243.
- Janz R, Sudhof TC, Hammer RE, Unni V, Siegelbaum SA, Bolshakov VY (1999) Essential roles in synaptic plasticity for synaptogyrin I and synaptophysin I. *Neuron* 24:687-700.
- Jung N, Haucke V (2007) Clathrin-mediated endocytosis at synapses. *Traffic* 8:1129-1136.
- Mallozzi C, Ceccarini M, Camerini S, Macchia G, Crescenzi M, Petrucci TC, Di Stasi AM (2009) Peroxynitrite induces tyrosine residue modifications in synaptophysin C-terminal domain, affecting its interaction with src. *J Neurochem* 111:859-869.
- McIntire SL, Reimer RJ, Schuske K, Edwards RH, Jorgensen EM (1997) Identification and characterization of the vesicular GABA transporter. *Nature* 389:870-876.
- McMahon HT, Bolshakov VY, Janz R, Hammer RE, Siegelbaum SA, Sudhof TC (1996) Synaptophysin, a major synaptic vesicle protein, is not essential for neurotransmitter release. *Proc Natl Acad Sci U S A* 93:4760-4764.
- Nakatsu F, Okada M, Mori F, Kumazawa N, Iwasa H, Zhu G, Kasagi Y, Kamiya H, Harada A, Nishimura K, Takeuchi A, Miyazaki T, Watanabe M, Yuasa S, Manabe T, Wakabayashi K, Kaneko S, Saito T, Ohno H (2004) Defective function of GABA-containing synaptic vesicles in mice lacking the AP-3B clathrin adaptor. *J Cell Biol* 167:293-302.
- Nonet ML (1999) Visualization of synaptic specializations in live *C. elegans* with synaptic vesicle protein-GFP fusions. *J Neurosci Methods* 89:33-40.
- Nonet ML, Saifee O, Zhao H, Rand JB, Wei L (1998) Synaptic transmission deficits in *Caenorhabditis elegans* synaptobrevin mutants. *J Neurosci* 18:70-80.
- Ruvinsky I, Ohler U, Burge CB, Ruvkun G (2007) Detection of broadly expressed neuronal genes in *C. elegans*. *Dev Biol* 302:617-626.
- Sandoval GM, Duerr JS, Hodgkin J, Rand JB, Ruvkun G (2006) A genetic interaction between the vesicular acetylcholine transporter VACHT/UNC-17 and synaptobrevin/SNB-1 in *C. elegans*. *Nat Neurosci* 9:599-601.
- Schmitt U, Tanimoto N, Seeliger M, Schaeffel F, Leube RE (2009) Detection of behavioral alterations and learning deficits in mice lacking synaptophysin. *Neuroscience* 162:234-243.
- Shaham S (2006) Glia-neuron interactions in the nervous system of *Caenorhabditis elegans*. *Curr*

- Opin Neurobiol 16:522-528.
- Shupliakov O (2009) The synaptic vesicle cluster: a source of endocytic proteins during neurotransmitter release. *Neuroscience* 158:204-210.
- Siebert A, Lottspeich F, Nelson N, Betz H (1994) Purification of the synaptic vesicle-binding protein physophilin. Identification as 39-kDa subunit of the vacuolar H(+)-ATPase. *J Biol Chem* 269:28329-28334.
- Sieburth D, Ch'ng Q, Dybbs M, Tavazoie M, Kennedy S, Wang D, Dupuy D, Rual JH, Hill DE, Vidal M, Ruvkun G, Kaplan JM (2005) Systematic analysis of genes required for synapse structure and function. *Nature* 436:510-517.
- Smith SM, Renden R, von Gersdorff H (2008) Synaptic vesicle endocytosis: fast and slow modes of membrane retrieval. *Trends Neurosci* 31:559-568.
- Song W, Zinsmaier KE (2003) Endophilin and synaptojanin hook up to promote synaptic vesicle endocytosis. *Neuron* 40:665-667.
- Spiwocks-Becker I, Vollrath L, Seeliger MW, Jaissle G, Eshkind LG, Leube RE (2001) Synaptic vesicle alterations in rod photoreceptors of synaptophysin-deficient mice. *Neuroscience* 107:127-142.
- Stenius K, Janz R, Sudhof TC, Jahn R (1995) Structure of synaptogyrin (p29) defines novel synaptic vesicle protein. *J Cell Biol* 131:1801-1809.
- Sugita S, Janz R, Sudhof TC (1999) Synaptogyrins regulate Ca²⁺-dependent exocytosis in PC12 cells. *J Biol Chem* 274:18893-18901.
- Takamori S et al. (2006) Molecular anatomy of a trafficking organelle. *Cell* 127:831-846.
- Tran MH, Yamada K, Nakajima A, Mizuno M, He J, Kamei H, Nabeshima T (2003) Tyrosine nitration of a synaptic protein synaptophysin contributes to amyloid beta-peptide-induced cholinergic dysfunction. *Mol Psychiatry* 8:407-412.
- Valtorta F, Pennuto M, Bonanomi D, Benfenati F (2004) Synaptophysin: leading actor or walk-on role in synaptic vesicle exocytosis? *Bioessays* 26:445-453.
- Vashlishan AB, Madison JM, Dybbs M, Bai J, Sieburth D, Ch'ng Q, Tavazoie M, Kaplan JM (2008) An RNAi screen identifies genes that regulate GABA synapses. *Neuron* 58:346-361.
- Verma R, Chauhan C, Saleem Q, Gandhi C, Jain S, Brahmachari SK (2004) A nonsense mutation in the synaptogyrin 1 gene in a family with schizophrenia. *Biol Psychiatry* 55:196-199.
- Williams SN, Locke CJ, Braden AL, Caldwell KA, Caldwell GA (2004) Epileptic-like convulsions associated with LIS-1 in the cytoskeletal control of neurotransmitter signaling in *Caenorhabditis elegans*. *Hum Mol Genet* 13:2043-2059.

Table 1: *C. elegans* strains

Strain	Genotype
BJ20	<i>wild type</i>
BJ14	<i>sng-1(ok234)X</i>
BJ23	<i>kcEx2[sng-1p::yfp]</i>
BJ31	<i>kcEx3[sng-1p::cfp]</i>
BJ60	<i>kcEx3[sng-1p::cfp]; oxIs12[lin-15(+), unc-47p::gfp], lin-15(n765ts)X</i>
BJ67	<i>eri-1(mg366)IV; sng-1(ok234)X</i>
BJ93	<i>snt-1(ed596)II; sng-1(ok234), oxIs12[lin-15(+), unc-47p::gfp], lin-15(n765ts)X</i>
BJ97	<i>chc-1(b1025ts)I; sng-1(ok234)X</i>
BJ98	<i>unc-64(e246)III; sng-1(ok234), oxIs12[lin-15(+), unc-47p::gfp], lin-15(n765ts)X</i>
BJ99	<i>unc-26(m2)IV; sng-1(ok234)X</i>
BJ100	<i>snb-1(md247)V; sng-1(ok234), oxIs12[lin-15(+), unc-47p::gfp], lin-15(n765ts)X</i>
BJ101	<i>unc-57(ok310)I; sng-1(ok234)X</i>
BJ103	<i>kcEx12[sng-1p::sng-1, ifb-2p::yfp]; sng-1(ok234)X</i>
BJ107	<i>kcEx8[sng-1::yfp]</i>
BJ109	<i>fat-3(wa22)IV; sng-1(ok234), oxIs12[lin-15(+), unc-47p::gfp], lin-15(n765ts)X</i>
BJ110	<i>unc-24(e138)IV; sng-1(ok234)X</i>
BJ115	<i>unc-57(e406)I; sng-1(ok234), oxIs12[lin-15(+), unc-47p::gfp], lin-15(n765ts)X</i>
BJ116	<i>unc-1(e538), sng-1(ok234), oxIs12[lin-15(+), unc-47p::gfp], lin-15(n765ts)X</i>
BJ117	<i>sng-1(ok234), dyn-1(ky51)X</i>
BJ118	<i>snt-1(nd290)II; sng-1(ok234)X</i>
BJ119	<i>snt-1(n2665)II; sng-1(ok234), oxIs12[lin-15(+), unc-47p::gfp], lin-15(n765ts)X</i>
BJ120	<i>kcEx19[sng-1p::sng-1, ifb-2p::yfp]</i>
BJ122	<i>snt-1(ed596)II; sng-1(ok234)X</i>
BJ123	<i>snt-1(n2665)II; sng-1(ok234)X</i>
BJ124	<i>snt-1(nd290)II; sng-1(ok234)X</i>
BJ125	<i>unc-57(ok310)I; sng-1(ok234)X</i>
BJ126	<i>unc-57(e406)I; sng-1(ok234)X</i>
BJ127	<i>unc-26(m2)IV; sng-1(ok234)X</i>
BJ174	<i>oxIs22[myo-3p::unc-49::gfp, lin-15(+)]II; sng-1(ok234)X</i>
BJ175	<i>nuls168[unc-129p::venus::rab-3, myo-2p::nls::gfp]IV; sng-1(ok234)X</i>
BJ176	<i>nuls152[unc-129p::gfp::snb-1, ttx-3p::mrfp]II; sng-1(ok234)X</i>
BJ178	<i>juls1[unc-25p::snb-1::gfp]IV; sng-1(ok234)X</i>
BJ180	<i>kcEx30[unc-25p::sng-1, ifb-2p::yfp]; sng-1(ok234)X</i>
BJ181	<i>kcEx30[unc-25p::sng-1, ifb-2p::yfp]; sng-1(ok234)X</i>
BJ182	<i>kcEx33[unc-25p::sng-1, ifb-2p::yfp]; juls1[unc-25p::snb-1::gfp]IV; sng-1(ok234)X</i>
BJ190	<i>kcEx31[unc-25p::sng-1, myo-3p::mcherry::unc-54]; sng-1(ok234)X</i>
BJ197	<i>kcEx34[unc-25p::sng-1, myo-2p::nls::gfp]; juls1[unc-25p::snb-1::gfp]IV; sng-1(ok234)X</i>
BX30	<i>fat-3(wa22)IV</i>
CB138	<i>unc-24(e138)IV</i>
CB406	<i>unc-57(e406)I</i>
CB538	<i>unc-1(e538)X</i>
CX51	<i>dyn-1(ky51)X</i>
CZ333	<i>juls1[unc-25p::snb-1::gfp]IV</i>
DA596	<i>snt-1(ed596)II</i>
DH1230	<i>chc-1(b1025ts)I</i>
DR2	<i>unc-26(m2)IV</i>
EG1055	<i>unc-64(e246)III</i>
EG1285	<i>oxIs12[lin-15(+), unc-47p::gfp], lin-15(n765ts)X</i>
EG1653	<i>oxIs22[myo-3p::unc-49::gfp, lin-15(+)]II</i>
EG2710	<i>unc-57(ok310)I</i>
EG3008	<i>sng-1(ok234), oxIs12[lin-15(+), unc-47p::gfp], lin-15(n765ts)X</i>
GR1373	<i>eri-1(mg366)IV</i>
KP3819	<i>nuls152[unc-129p::gfp::snb-1, ttx-3p::mrfp]II</i>
KP3961	<i>nuls168[unc-129p::venus::rab-3, myo-2p::nls::gfp]IV</i>
MT6977	<i>snt-1(n2665)II</i>
N2	<i>wild type</i>
NM204	<i>snt-1(nd290)II</i>
NM467	<i>snb-1(md247)V</i>
VH180	<i>hdEx24[rol-6(su1006), sng-1::yfp]</i>

Table 1: *C. elegans* strains

Strain	Genotype
BJ20	<i>wild type</i>
BJ14	<i>sng-1(ok234)X</i>
BJ23	<i>kcEx2[sng-1p::yfp]</i>
BJ31	<i>kcEx3[sng-1p::cfp]</i>
BJ60	<i>kcEx3[sng-1p::cfp]; oxIs12[lin-15(+), unc-47p::gfp], lin-15(n765ts)X</i>
BJ67	<i>eri-1(mg366)IV; sng-1(ok234)X</i>
BJ93	<i>snt-1(ed596)II; sng-1(ok234), oxIs12[lin-15(+), unc-47p::gfp], lin-15(n765ts)X</i>
BJ97	<i>chc-1(b1025ts)I; sng-1(ok234)X</i>
BJ98	<i>unc-64(e246)III; sng-1(ok234), oxIs12[lin-15(+), unc-47p::gfp], lin-15(n765ts)X</i>
BJ99	<i>unc-26(m2)IV; sng-1(ok234)X</i>
BJ100	<i>snb-1(md247)V; sng-1(ok234), oxIs12[lin-15(+), unc-47p::gfp], lin-15(n765ts)X</i>
BJ101	<i>unc-57(ok310)I; sng-1(ok234)X</i>
BJ103	<i>kcEx12[sng-1p::sng-1, ifb-2p::yfp]; sng-1(ok234)X</i>
BJ107	<i>kcEx8[sng-1::yfp]</i>
BJ109	<i>fat-3(wa22)IV; sng-1(ok234), oxIs12[lin-15(+), unc-47p::gfp], lin-15(n765ts)X</i>
BJ110	<i>unc-24(e138)IV; sng-1(ok234)X</i>
BJ115	<i>unc-57(e406)I; sng-1(ok234), oxIs12[lin-15(+), unc-47p::gfp], lin-15(n765ts)X</i>
BJ116	<i>unc-1(e538), sng-1(ok234), oxIs12[lin-15(+), unc-47p::gfp], lin-15(n765ts)X</i>
BJ117	<i>sng-1(ok234), dyn-1(ky51)X</i>
BJ118	<i>snt-1(nd290)II; sng-1(ok234)X</i>
BJ119	<i>snt-1(n2665)II; sng-1(ok234), oxIs12[lin-15(+), unc-47p::gfp], lin-15(n765ts)X</i>
BJ120	<i>kcEx19[sng-1p::sng-1, ifb-2p::yfp]</i>
BJ122	<i>snt-1(ed596)II; sng-1(ok234)X</i>
BJ123	<i>snt-1(n2665)II; sng-1(ok234)X</i>
BJ124	<i>snt-1(nd290)II; sng-1(ok234)X</i>
BJ125	<i>unc-57(ok310)I; sng-1(ok234)X</i>
BJ126	<i>unc-57(e406)I; sng-1(ok234)X</i>
BJ127	<i>unc-26(m2)IV; sng-1(ok234)X</i>
BJ174	<i>oxIs22[myo-3p::unc-49::gfp, lin-15(+)]II; sng-1(ok234)X</i>
BJ175	<i>nuls168[unc-129p::venus::rab-3, myo-2p::nls::gfp]IV; sng-1(ok234)X</i>
BJ176	<i>nuls152[unc-129p::gfp::snb-1, ttx-3p::mrfp]II; sng-1(ok234)X</i>
BJ178	<i>juls1[unc-25p::snb-1::gfp]IV; sng-1(ok234)X</i>
BJ180	<i>kcEx30[unc-25p::sng-1, ifb-2p::yfp]; sng-1(ok234)X</i>
BJ181	<i>kcEx30[unc-25p::sng-1, ifb-2p::yfp]; sng-1(ok234)X</i>
BJ182	<i>kcEx33[unc-25p::sng-1, ifb-2p::yfp]; juls1[unc-25p::snb-1::gfp]IV; sng-1(ok234)X</i>
BJ190	<i>kcEx31[unc-25p::sng-1, myo-3p::mcherry::unc-54]; sng-1(ok234)X</i>
BJ197	<i>kcEx34[unc-25p::sng-1, myo-2p::nls::gfp]; juls1[unc-25p::snb-1::gfp]IV; sng-1(ok234)X</i>
BX30	<i>fat-3(wa22)IV</i>
CB138	<i>unc-24(e138)IV</i>
CB406	<i>unc-57(e406)I</i>
CB538	<i>unc-1(e538)X</i>
CX51	<i>dyn-1(ky51)X</i>
CZ333	<i>juls1[unc-25p::snb-1::gfp]IV</i>
DA596	<i>snt-1(ed596)II</i>
DH1230	<i>chc-1(b1025ts)I</i>
DR2	<i>unc-26(m2)IV</i>
EG1055	<i>unc-64(e246)III</i>
EG1285	<i>oxIs12[lin-15(+), unc-47p::gfp], lin-15(n765ts)X</i>
EG1653	<i>oxIs22[myo-3p::unc-49::gfp, lin-15(+)]II</i>
EG2710	<i>unc-57(ok310)I</i>
EG3008	<i>sng-1(ok234), oxIs12[lin-15(+), unc-47p::gfp], lin-15(n765ts)X</i>
GR1373	<i>eri-1(mg366)IV</i>
KP3819	<i>nuls152[unc-129p::gfp::snb-1, ttx-3p::mrfp]II</i>
KP3961	<i>nuls168[unc-129p::venus::rab-3, myo-2p::nls::gfp]IV</i>
MT6977	<i>snt-1(n2665)II</i>
N2	<i>wild type</i>
NM204	<i>snt-1(nd290)II</i>
NM467	<i>snb-1(md247)V</i>
VH180	<i>hdEx24[rol-6(su1006), sng-1::yfp]</i>

Table 2:

Measurements of synaptic density and synaptic width using different fluorescent markers.

Marker	Genotype	Strain	Density per 10 μm	Width [μm]
<i>juIs1[unc-25p::snb-1::gfp]</i>	<i>wt</i>	CZ333	2.81 \pm 0.10	1.18 \pm 0.02
	<i>sng-1</i>	BJ178	2.60 \pm 0.06, P=0.07	1.31 \pm 0.04, P=0.005
<i>nuIs152[unc-129p::gfp::snb-1]</i>	<i>wt</i>	KP3819	2.89 \pm 0.13	1.00 \pm 0.04
	<i>sng-1</i>	BJ176	2.84 \pm 0.08, P=0.6	1.17 \pm 0.03, P=0.0007
<i>nuIs168[unc-129p::venus::rab-3]</i>	<i>wt</i>	KP3961	3.18 \pm 0.11	0.82 \pm 0.03
	<i>sng-1</i>	BJ175	3.04 \pm 0.06, P=0.3	0.91 \pm 0.02, P=0.07
<i>oxIs22[myo-3p::unc-49::gfp]</i>	<i>wt</i>	EG1653	2.94 \pm 0.06	0.95 \pm 0.03
	<i>sng-1</i>	BJ174	3.07 \pm 0.05, P=0.09	1.07 \pm 0.04, P=0.01

Figure 1

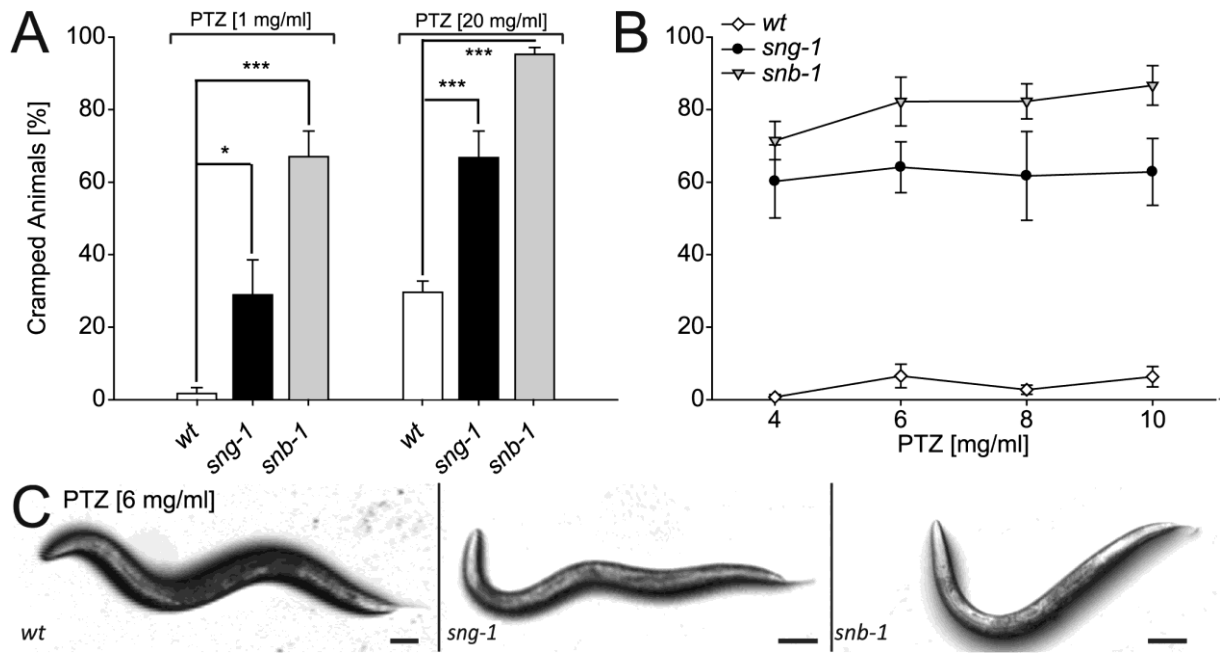


Figure 2

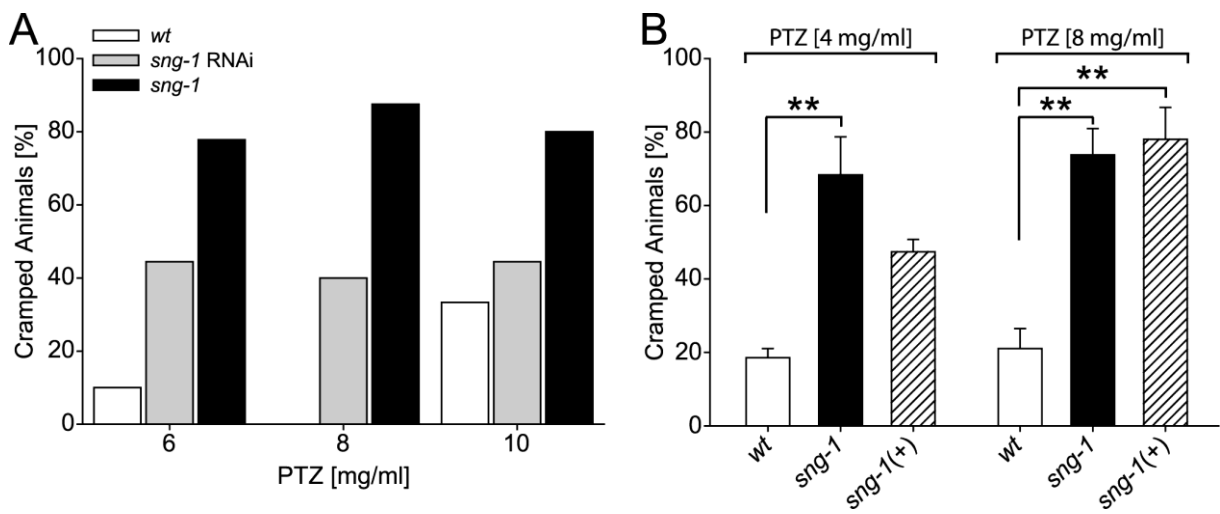


Figure 3

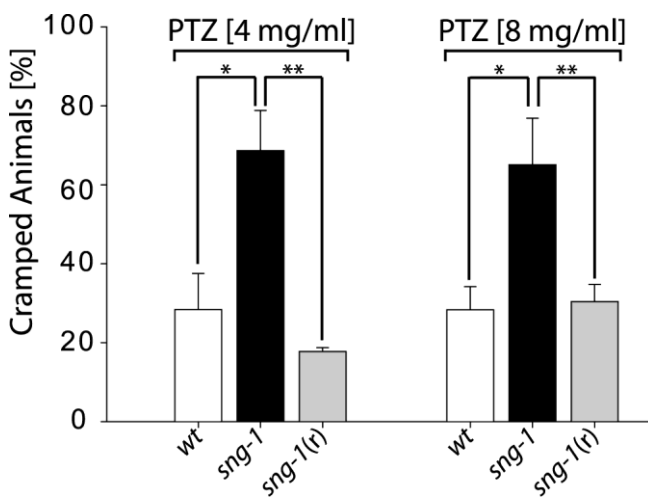


Figure 4

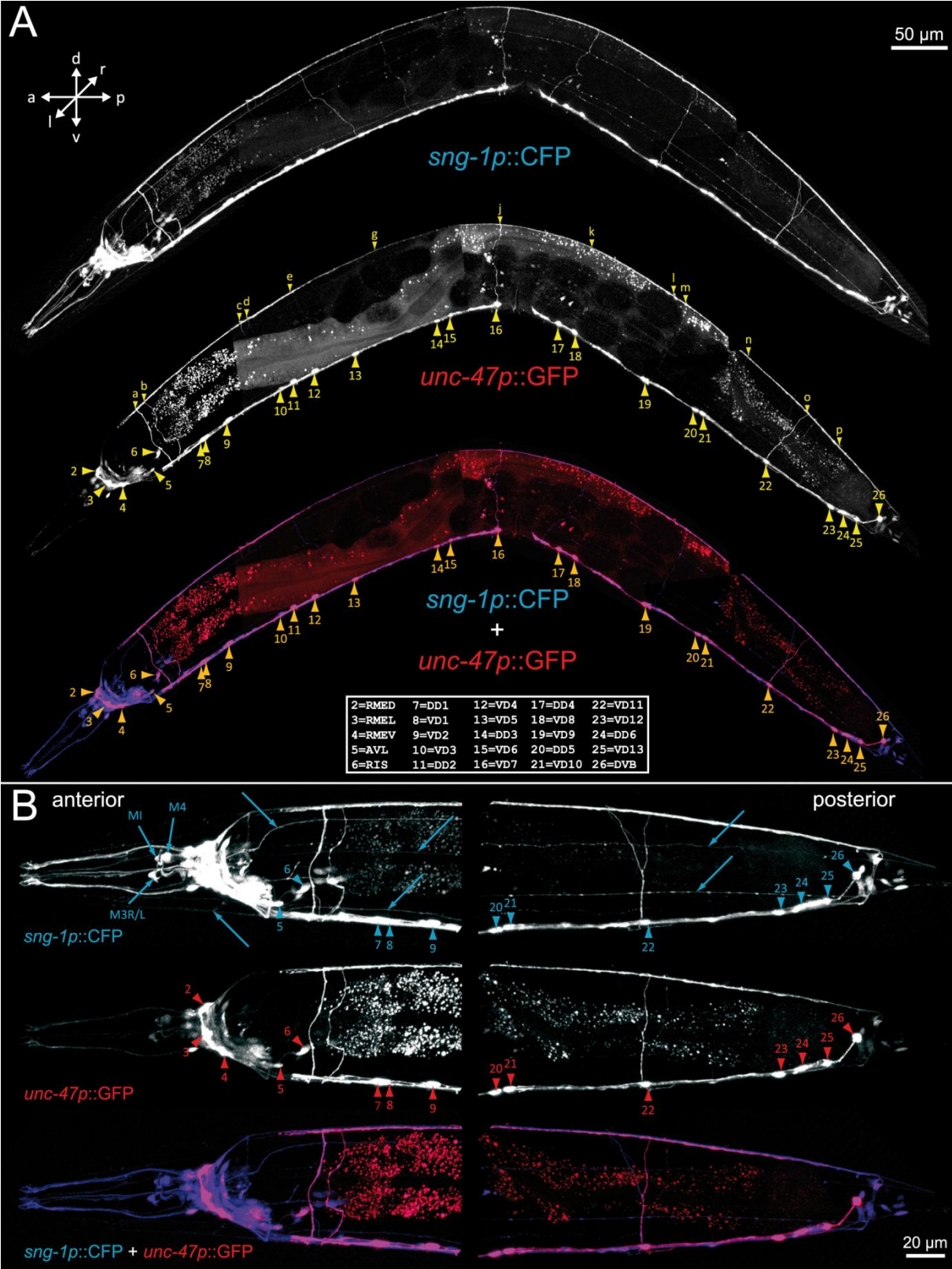


Figure5

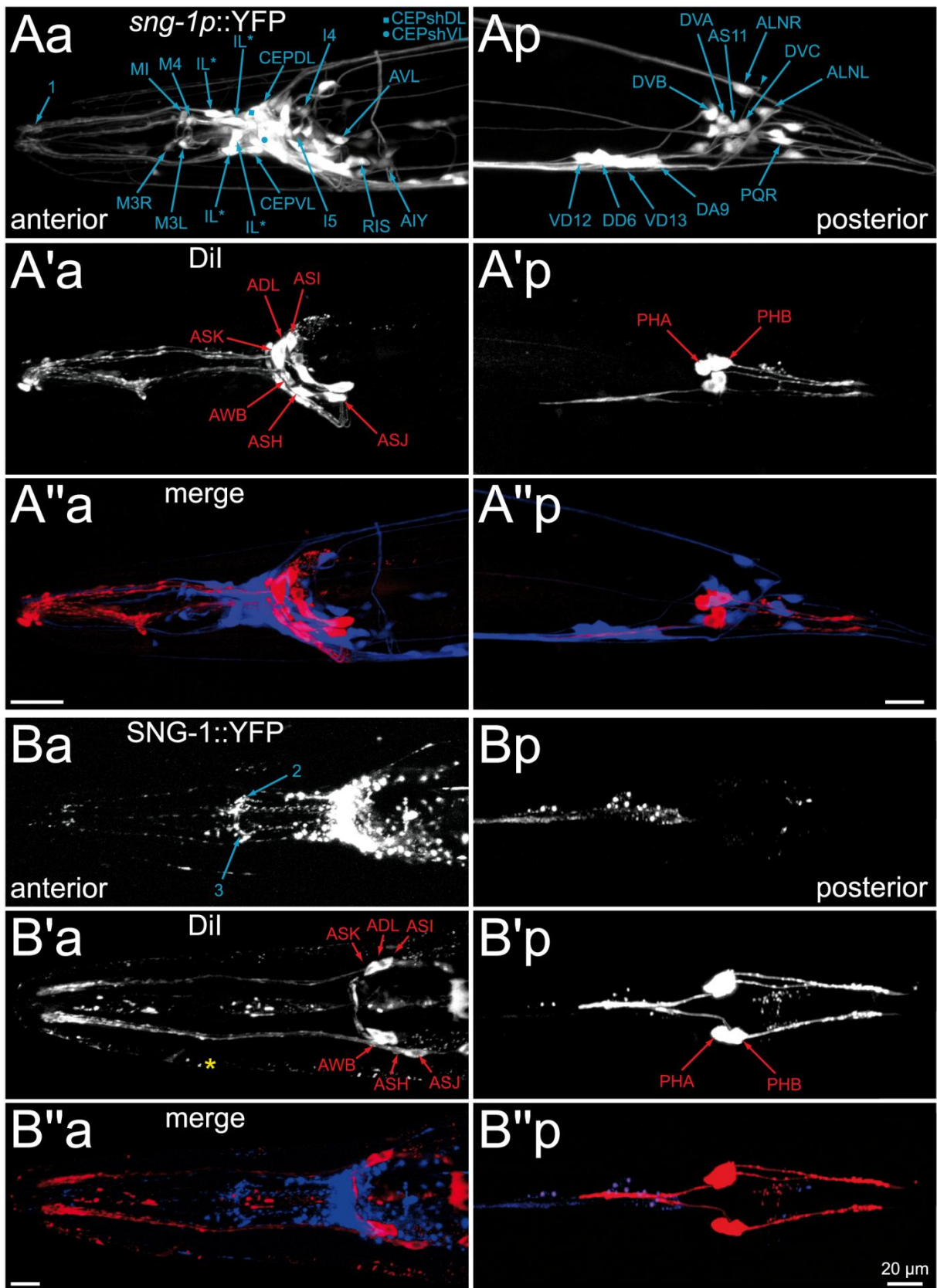


Figure 6

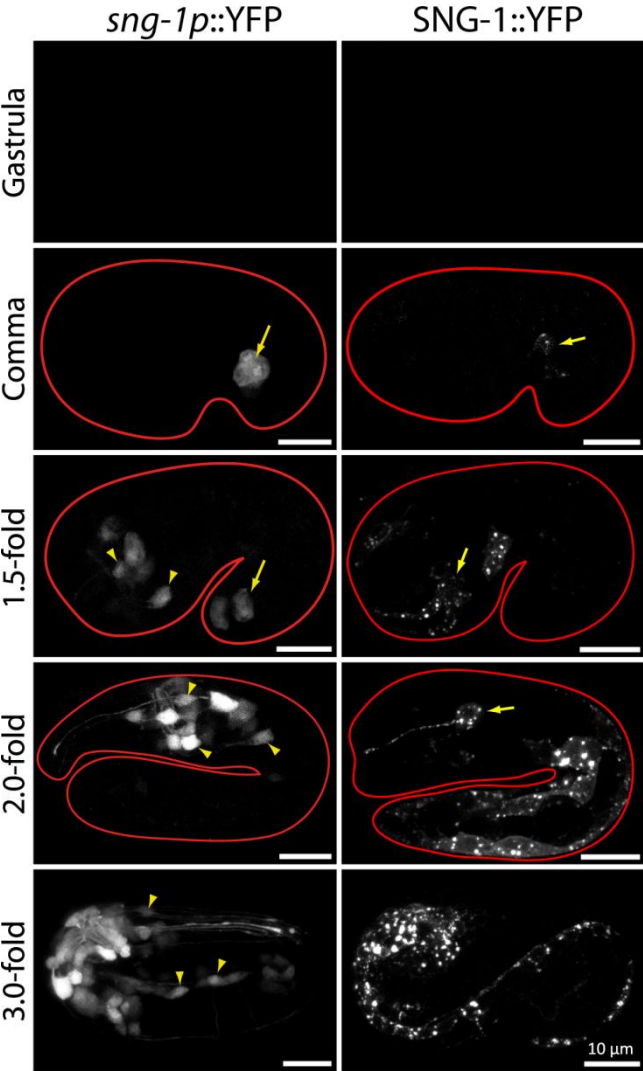


Figure 7

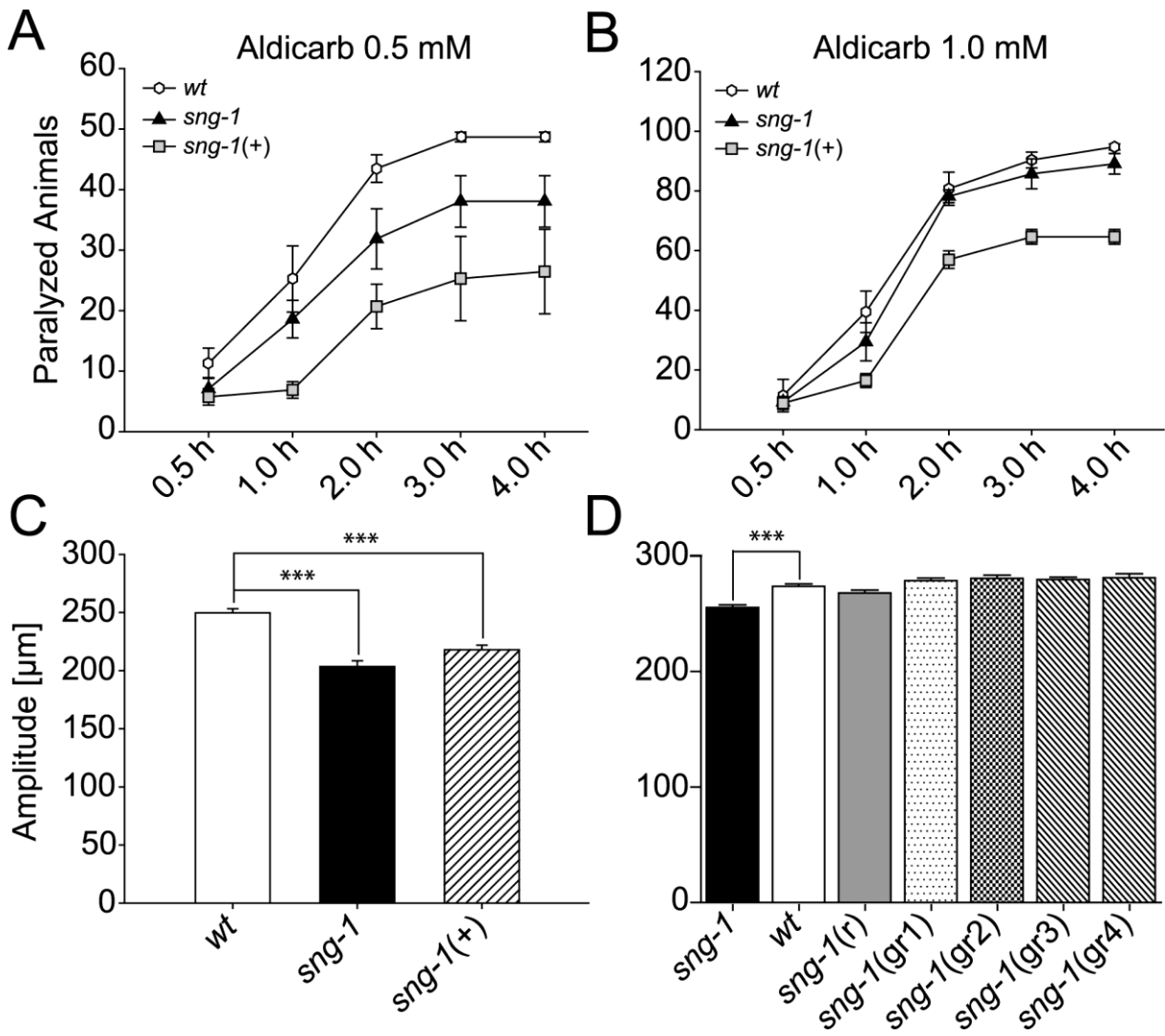
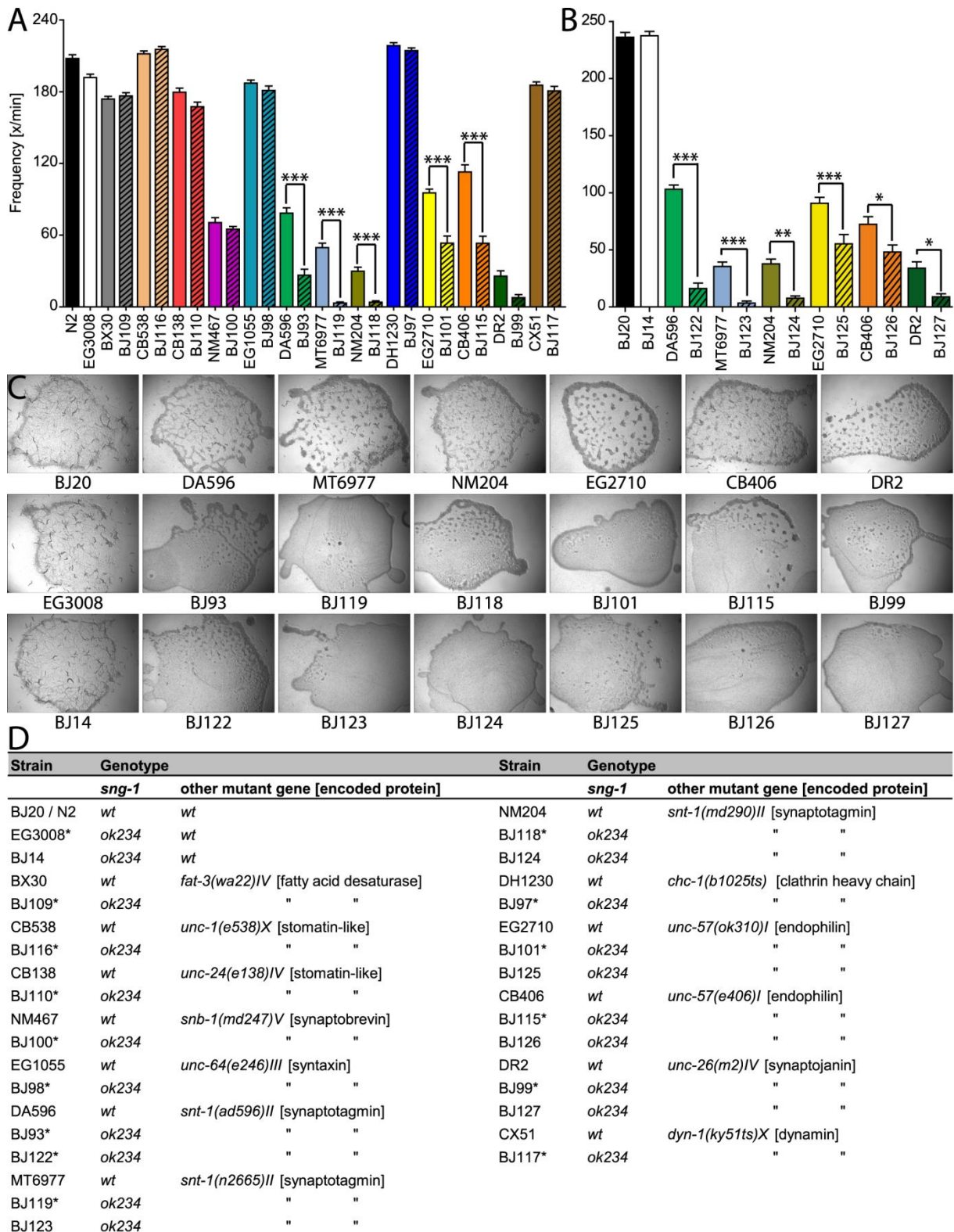


Figure 8



*These strains also contain *oxIs12 [lin-15(+), unc-47p::gfp]*